



## Polyethyleneimine functionalized magnetic nanocluster for removal of heavy metal ions in water

Kyu Sun Hwang<sup>a,b</sup>, Chan Woo Park<sup>a</sup>, Kune-Woo Lee<sup>a</sup>, Bum-Kyoung Seo<sup>a</sup>, So-Jin Park<sup>b,\*</sup>, Hee-Man Yang<sup>a,\*</sup>

<sup>a</sup>Decontamination & Decommissioning Research Division, Korea Atomic Energy Research Institute, 989-111 Daedukdaero, Yuseong, Daejeon, 305-353, Republic of Korea; Tel. +82-42-868-8269 (H.-M. Yang); +82-42-821-5684 (S.-J. Park); Fax: +82-42-868-8667 (H.-M. Yang); email: hmyang@kaeri.re.kr (H.-M. Yang); sjpark@cnu.ac.kr (S.-J. Park);

<sup>b</sup>Department of Chemical engineering, Chungnam National University, Daejeon, 305-764, Republic of Korea

Received 23 December 2015; Accepted 9 May 2016

### ABSTRACT

Polyethyleneimine (PEI) functionalized magnetic nanoclusters (MNCs) were fabricated for the removal of heavy metal ions and rapid magnetic separation of adsorbent from contaminated water. After the MNCs, composed of aggregates of small primary  $\text{Fe}_3\text{O}_4$  nanoparticles with a size of 6.2 nm, were synthesized by one-step hydrothermal method, they were covalently coated with PEI via a simple silane coupling reaction. The resulting PEI-functionalized MNCs (PEI-MNC) had an average diameter of 264.1 nm and showed rapid separation from water by an external magnet. The adsorption behavior of PEI-MNC for heavy metal ions fits well with the Langmuir isotherm models, and their maximum adsorption capacity was 33.11, 11.05, and 9.80 mg/g for  $\text{Cu}^{2+}$ ,  $\text{Zn}^{2+}$ , and  $\text{Co}^{2+}$ , respectively. Competitive adsorption among these three metal ions was carried out to investigate the adsorption tendency of PEI-MNC between them. Furthermore, the desorption and stability test of  $\text{Cu}^{2+}$ -loaded PEI-MNC in 0.1 M HCl were also investigated to evaluate their reusability for practical application.

**Keywords:** Polyethyleneimine; Magnetic nanocluster; Magnetic separation; Heavy metal ions

### 1. Introduction

Heavy metals pollution commonly found in wastewater of many industrial processes has been a serious threat to the public health and ecological systems due to their properties of nonbiodegradation, potential toxicity, and carcinogenesis even at very low concentrations [1]. Among the methods for heavy metal pollution remediation, such as adsorption, electrochemical precipitation, ion exchange, and membrane filtration, adsorption is one of the most popular and effective options due to its great flexibility in design and operation. Up to now, various adsorbents such as natural materials like clay, seaweed, and biomass, as well as synthetic materials adsorbents like activated carbon, resin, and mesoporous silica have been used to remove heavy metals [2,3]. Although these adsorbents can

be regenerated and/or recovered using the centrifugation or filtration method, however, they are difficult to be separated from large volumes of solution [4].

In recent decades, magnetic nanoparticles (MNPs), such as  $\text{Fe}_3\text{O}_4$ , have been extensively studied for their utility in environmental remediation applications, magnetically guided drug delivery, and magnetic resonance imaging, due to their unique superparamagnetic and biocompatible properties [5,6]. In particular, magnetic nanocomposites composed of a MNP-based core and a functional shell that can adsorb contaminants such as organic pollutants [4] and radioactive nuclides [7–9] were intensively studied for the treatment of contaminated water because they can be magnetically collected using an external magnet. Moreover, a variety of magnetic nanoadsorbents functionalized with various compounds, such as alginate [10], chitosan [11], hexanediamine [12], amino-functionalized polyacrylic acid (PAA) [13], and dimercaptosuccinic acid [14], have been developed for the removal of heavy metal ions. Among these

\* Corresponding author.

various coating compounds, polyethyleneimine (PEI), composed of a large number of primary and secondary amine groups, is well known to have outstanding adsorption ability for heavy metals such as Cu ions [8,15]. For instance, Goon et al. and Pang et al. recently reported that PEI-coated MNPs have good adsorption capacity for Cu<sup>2+</sup> ions [16] or Cr<sup>2+</sup> ions [17]. However, these PEI-coated MNPs, prepared through electrostatic conjugation between Fe<sub>3</sub>O<sub>4</sub> and PEI, can become unstable at high or low pH, and under certain conditions of high salt.

In the present study, MNC, composed of aggregates of small primary Fe<sub>3</sub>O<sub>4</sub> nanoparticles, was used as a core materials in magnetic adsorbent to provide a much higher saturation magnetization than individual Fe<sub>3</sub>O<sub>4</sub> nanoparticles due to aggregation effects [18,19]. PEI was then covalently conjugated on the surface of MNC using PEI-silane (trimethoxysilylpropyl-modified PEI) via simple silane coupling reaction to improve the structural stability. The structure, morphology, and magnetic properties of the resulting PEI-MNC were characterized by X-ray diffraction (XRD), Fourier transform infrared (FTIR), Transmission electron microscopy (TEM), and vibrating sample magnetometer (VSM). The adsorption capability of PEI-MNC in removing heavy metal ions such as Cu<sup>2+</sup>, Co<sup>2+</sup>, and Zn<sup>2+</sup> from water was also investigated by measuring adsorption isotherm in batch experiments. Moreover, stability of the PEI-MNC during desorption process in 0.1 M HCl was examined

## 2. Materials and methods

### 2.1. Synthesis of citric acid-coated magnetic nanocluster

Citric acid (CA) coated MNCs (CA-MNCs) were synthesized using a reported procedure [20]. Briefly, 2.7 g of FeCl<sub>3</sub>·6H<sub>2</sub>O, 0.8 g of sodium citric acid, and 7.708 g of ammonium acetate were dissolved in 140 mL of ethylene glycol under magnetic stirring. Then, the mixture solution was transferred into a Teflon-lined stainless-steel autoclave. The autoclave was sealed and heated to 200°C for 6 h. After being cooled to room temperature, the produced were obtained with the help of magnet, washed with excess ethanol and deionized water for several times, and dried in vacuum at 60°C for overnight.

### 2.2. Synthesis of polyethyleneimine (PEI) functionalized magnetic nanoclusters

PEI-MNC was fabricated according to the previously reported literature with modification [21]. Briefly, 100 mg of CA-MNC were dispersed in 50 mL of ethanol-water mixture solution (the volume ratio of ethanol and water is 4 to 1). Then 1 mL of PEI-silane (trimethoxysilylpropyl-modified PEI [TMS-PEI]; Molecular weight (MW) = 1,500–1,800, Gelest, Inc., Morrisville, PA) and 1.5 mL of ammonium hydroxide solution (28.0%–30.0% NH<sub>3</sub> basis) were added to upper solution. The suspension was stirred violently at 80°C for 24 h. After being cooled to room temperature, the PEI-MNC was separated from solution by a permanent magnet and washed with excess ethanol and water several times. Finally, the product was dried in vacuum at 60°C for overnight.

### 2.3. Characterization of CA-MNC and PEI-MNC

TEM) was obtained using a Philips CM-200 instrument operating at 200 kV. Nanoparticle sizes were measured by

dynamic light scattering (DLS) instrument (ELS-Z2, particle size analyzer and zeta potential, Otsuka Electronics Co. Ltd., Japan). FTIR spectra were recorded using a Spectrum GX and Auto Image instrument (PerkinElmer, Shelton, CT, USA) at room temperature. Spectra were recorded in the range of 4,000–550 cm<sup>-1</sup>. The thermal gravimetric analysis (TGA) was carried out on a SETSYS 16/18 (Setaram, France). The saturation of magnetization was evaluated using a VSM (model 955287(A), Lakeshore, Westerville, OH, USA).

### 2.4. Adsorption and desorption studies

The adsorption of various transition metals such as Cu<sup>2+</sup>, Co<sup>2+</sup>, and Zn<sup>2+</sup> by PEI-MNC was performed at 25°C. 5 mg of PEI-MNC were mixed with 50 mL of aqueous solution containing various concentration of Cu<sup>2+</sup>, Co<sup>2+</sup>, or Zn<sup>2+</sup> at pH 7. The initial concentration of them was varied from 0.1 to 50 ppm. After shaking the mixture solution for 24 h to reach adsorption equilibrium, the PEI-MNC was separated with the help of a magnet. The initial and residual concentration of various transition metal ions in water before and after treatment with PEI-MNCs were measured by inductively coupled plasma atomic emission spectrometer (ICP-AES; model: OPTMA 7300DV, PerkinElmer, Shelton, CT, USA). The amount of heavy metal ions adsorbed at equilibrium ( $q_e$ ) was given according to the formula:

$$q_e = (c_0 - c_e) \times V/m \quad (1)$$

where  $c_0$  and  $c_e$  (mg/L) are the initial and equilibrium concentration of metal ions in solution;  $V$  is the volume of the solution; and  $m$  (g) is the mass of PEI-MNC. To survey the competitive adsorption among Cu<sup>2+</sup>, Zn<sup>2+</sup>, and Co<sup>2+</sup>, 5 mg of PEI-MNC were added into 50 mL multi-metal solution with the initial pH 6. For tri-metal solution, the concentration was 5 ppm for each metal.

Desorption of Cu<sup>2+</sup> was performed by mixing the Cu<sup>2+</sup>-loaded PEI-MNC (10 mg) into 100 mL of HCl solution (0.1 mol/L), and sonicating for various time (from 2 min to 1 h). Then, the PEI-MNC was separated from the solution with the help of a magnet. The amount of Cu in the Cu<sup>2+</sup>-loaded PEI-MNC before desorption test and the released concentration of Cu<sup>2+</sup> from the Cu<sup>2+</sup>-loaded PEI-MNC in water during desorption test were measured using an ICP-AES (model: OPTMA 7300DV, PerkinElmer, Shelton, CT, USA).

## 3. Results and discussion

The procedure used to synthesize the PEI-MNC for removal of heavy metal ions is illustrated in Fig. 1. First, the MNC was synthesized via a hydrothermal reaction of FeCl<sub>3</sub>·6H<sub>2</sub>O with ammonium acetate and sodium citrate acid (CA) in ethylene glycol [20]. The morphology of CA-MNCs is shown in the TEM image. As shown in Fig. 2, the obtained CA-MNC had a spherical shape with a mean diameter of about 200 nm. A TEM image further reveals that the microspheres are composed of nanocrystals with a size of about 5–8 nm. The crystalline structure of CA-MNC was determined by the XRD as shown in Fig. 3. XRD analysis showed that six characteristic peaks at about  $2\theta = 30.2^\circ$ ,  $36.6^\circ$ ,  $43.1^\circ$ ,  $53.4^\circ$ ,  $57.1^\circ$  and  $62.7^\circ$ , corresponded to the (2 2 0), (3 1 1), (4 0 0), (4 2 2), (5 1 1) and (4 4 0) phase of Fe<sub>3</sub>O<sub>4</sub>,

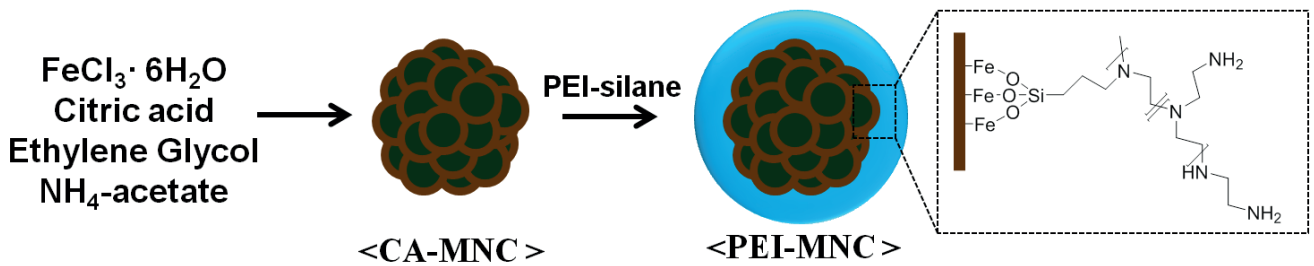


Fig. 1. The synthetic procedure of PEI-MNC for the removal of heavy metal ions.

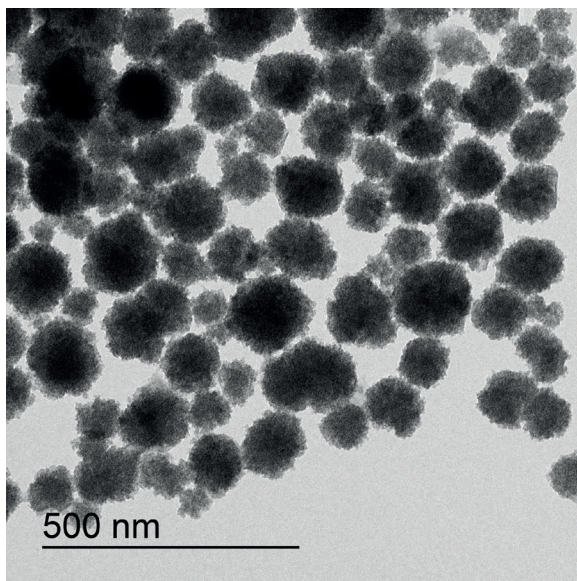


Fig. 2. TEM images of CA-MNC.

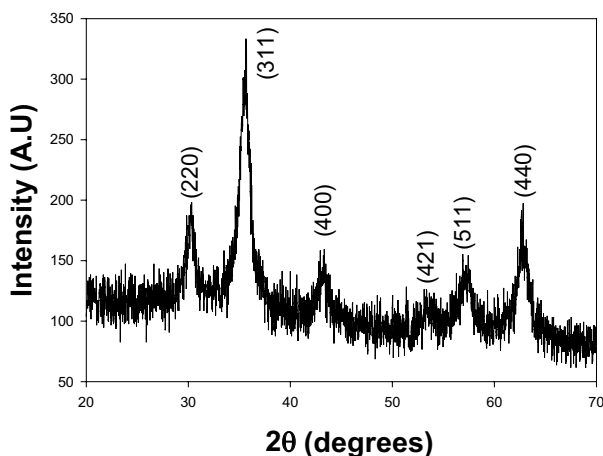


Fig. 3. X-ray diffraction patterns of CA-MNC using a Rigaku D/max-RB apparatus and a Cu K $\alpha$  source ( $\lambda = 0.154$  nm).

respectively, indicating that CA-MNC consisted of a Fe<sub>3</sub>O<sub>4</sub> phase [9]. The average crystallite size in these microspheres can be further calculated by the strongest peak at 30.2° in the XRD spectrum (Fig. 3) using Scherrer's formula; the data were around 6.2 nm, consistent with the TEM result.

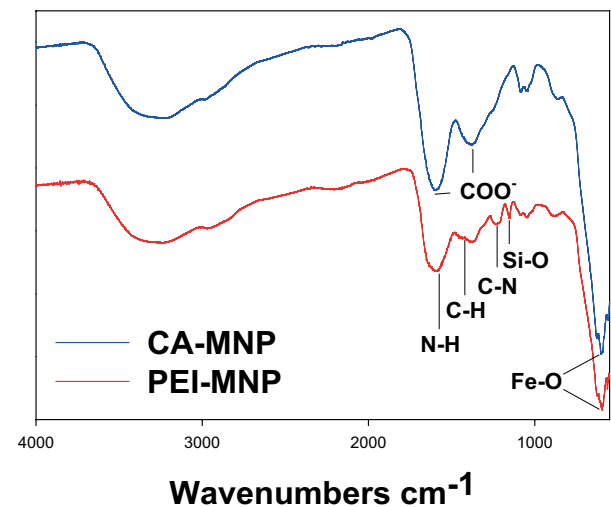


Fig. 4. FTIR spectra of CA-MNC and PEI-MNC.

The FTIR spectra of CA-MNC were examined to verify the capping ligand on the surface of nanoparticles (Fig. 4). In the spectrum of CA-MNC, the strong band observed at around 598 cm<sup>-1</sup> can be ascribed to the Fe–O stretching vibrational mode of Fe<sub>3</sub>O<sub>4</sub> [9], while the presence of peaks at 1,602 cm<sup>-1</sup> for carboxylate symmetric stretching and 1,382 cm<sup>-1</sup> for carboxylate antisymmetric stretching are associated with sodium citrate. This result indicated that sodium citrate was bonded on the surface of MNC covalently through the interaction between the carboxylate group of citrate and the Fe atom [20,22]. The hydrodynamic diameter of the CA-MNC in water determined by DLS was 218.6 ± 70.99 nm, consistent with the TEM result. The zeta potential value of the MNC in water was (-) 28.6 ± 0.89 mV. This value was attributed to the unbound carboxylate groups in CA on the surface of CA-MNC.

PEI-silane was used to modify the surface of CA-MNC through covalent attachment of the functional alkoxy silanes, thereby simultaneously conjugation of PEI on the surface of CA-MNC for the adsorption of heavy metal in water because it is well known that PEI have outstanding adsorption ability for heavy metal [2,15]. During the reaction between the iron atom on the CA-MNC surface and the PEI-silanes, the methoxy groups of the PEI-silane easily hydrolyzed to form an Fe–O–Si bond with the Fe atoms on the surface of MNC [7,21,23]

The surface modification of the CA-MNC with PEI-silane, termed PEI-MNC, was confirmed by the FTIR spectrum of



PEI-MNC. In Fig. 4, the PEI-MNC also has the characteristic peak of  $\text{Fe}_3\text{O}_4$  at  $598\text{ cm}^{-1}$  corresponding to the Fe–O stretching vibration. Besides, the PEI-MNC has the characteristic peaks of PEI-silane at  $1,046\text{ cm}^{-1}$  corresponding to the stretching vibrations of the Si–O–Si bond, at  $1,570\text{ cm}^{-1}$  for N–H bending of PEI, at  $1,445\text{ cm}^{-1}$  for C–H bending of PEI, and at  $1,241\text{ cm}^{-1}$  for C–N stretching of PEI. This result indicates that the PEI-silane was successfully conjugated onto the surface of MNC [24,17].

The fabricated PEI-MNC was found to be stable in aqueous solutions without any agglomeration phenomenon. The hydrodynamic diameter of the PEI-MNC in water, determined by DLS was  $264.1 \pm 84.45\text{ nm}$  (Fig. 5). From the above result, the increased mean diameter of PEI-MNC compared with that of CA-MNC demonstrated the presence of PEI on the surface of CA-MNC. The zeta potential value in water was reversibly changed from  $(-)$   $28.6 \pm 0.89\text{ mV}$  for CA-MNC to  $(+)$   $37.0 \pm 0.61\text{ mV}$  for PEI-MNC. This is attributed to the presence of the amine groups of PEI on the surface of PEI-MNC, similar to the other reported formulation [8].

The amounts of  $\text{Fe}_3\text{O}_4$  in CA-MNC and PEI-MNC, and the amount of PEI in PEI-MNC were measured using a TGA. After the organic components in CA-MNC and PEI-MNC had completely decomposed upon heating to  $800^\circ\text{C}$ , the residual substance was mainly  $\text{Fe}_3\text{O}_4$ . Fig. 6 shows that the weight percentage of the  $\text{Fe}_3\text{O}_4$  in CA-MNC and PEI-MNC were 83.69% and 69.86%, respectively.

The magnetic properties of CA-MNC and PEI-MNC were examined using a VSM. The plots of magnetization vs. magnetic field at room temperature for CA-MNC and PEI-MNC are illustrated in Fig. 7. Both samples showed superparamagnetic behaviors and the saturation magnetizations ( $M_s$  value) of the CA-MNC and PEI-MNC were  $57.94$  and  $48.71\text{ emu g}^{-1}$ , respectively. Although the  $M_s$  value of PEI-MNC is lower than that of CA-MNC due to the presence of PEI which do not have any magnetic property, the normalized  $M_s$  value ( $69.73\text{ emu g}^{-1}$ ) for the PEI-MNC from TGA results was almost equal to the value of the original value for the  $\text{Fe}_3\text{O}_4$  ( $69.23\text{ emu g}^{-1}$ ) obtained from the CA-MNC, indicating that the grafting of PEI on the surface of MNC did not change the magnetic property of the magnetite. The magnetic separation ability of PEI-MNC by an external magnet is demonstrated in Fig. 8. After placing the external magnet on one side of the bottle, the PEI-MNC has been collected to the side close to magnet. This vivid phenomenon clearly confirmed that the PEI-MNC could be easily separated from water by an external magnet.

It is well known that adsorption mechanism of heavy metal ions ( $M^{n+}$ ) on the surface of amino-functionalized nanoparticles is the formation of complexes ( $\text{NH}_2M^{n+}$ ) of metal ions with the amino groups at solid at the solid–solution interface of amino-functionalized nanoparticles [12,14]. However, the formation of complexes ( $\text{NH}_2M^{n+}$ ) is significantly influenced by the pH value because the protonation of amine groups ( $\text{NH}_3^+$ ) at lower pH causes the loss of  $\text{NH}_2$  binding sites on the surface of PEI-MNC for metal ions adsorption [14]. Moreover, the  $\text{NH}_3^+$  formed on the surface of PEI-MNC at lower pH hinders the metal ions from contacting the PEI-MNC surface by the strong electrostatic repulsion force. Fig. 9 shows pH dependent zeta-potential value of PEI-MNC at room temperature. Although the pH of zero

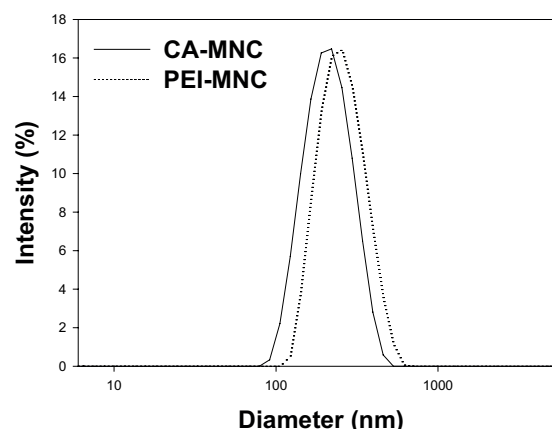


Fig. 5. Size distribution for CA-MNC and PEI-MNC in water.

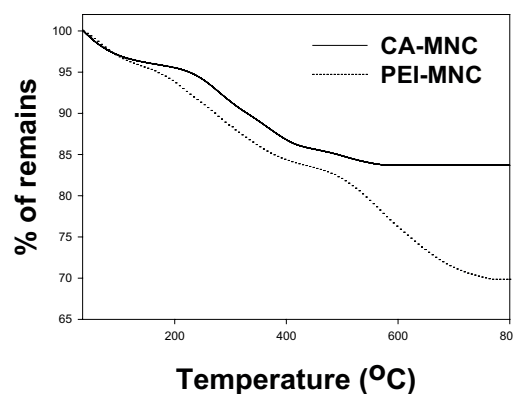


Fig. 6. TGA curves of the CA-MNC and PEI-MNC.

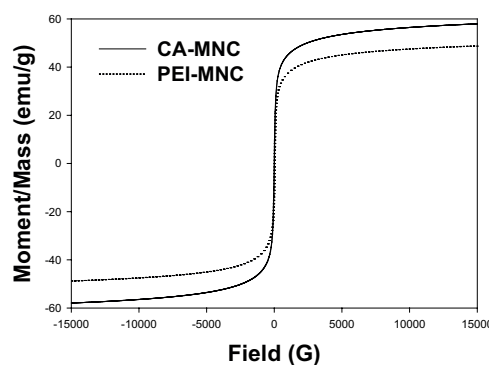


Fig. 7. Magnetization curves of CA-MNC and PEI-MNC.

point charge ( $\text{pH}_{\text{pzc}}$ ) of PEI-MNC was found to be around 8.95, the positive surface charge of PEI-MNC decreased as the solution pH increased. From the electrostatic interaction point of view, the adsorption of metal ions can be increased as the solution pH increased by weak electrostatic repulsion force. Taking into further consideration, the occurrence of metal hydroxide precipitation under high pH solution [25], pH at 7 was selected for effective adsorption of heavy metals such as  $\text{Co}^{2+}$ ,  $\text{Zn}^{2+}$ , and  $\text{Cu}^{2+}$  in this work.

The adsorption capacities of the PEI-MNC to heavy metal ions at pH 7 were examined by measuring adsorption

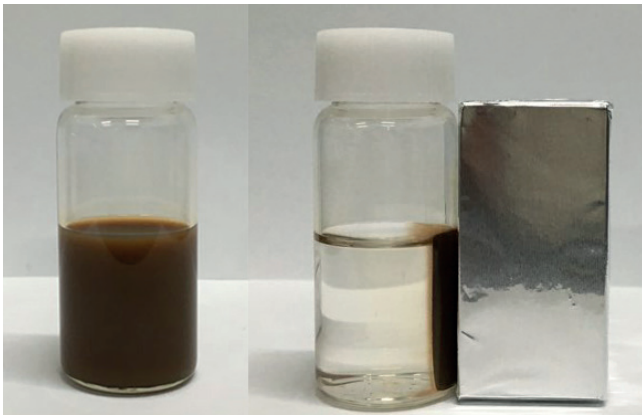


Fig. 8. A well-mixed PEI-MNC solution in the absence of an external magnet (left), and the separated solution after placing a magnet adjacent to the original well-mixed PEI-MNC solution (right).

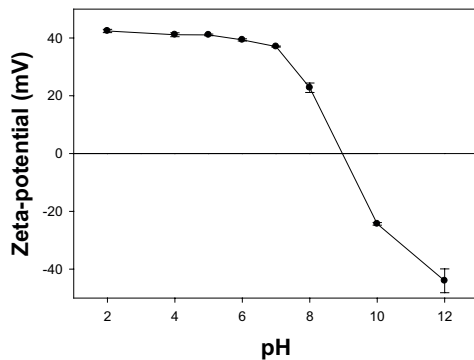


Fig. 9. Zeta potentials of PEI-MNC at various pH values.

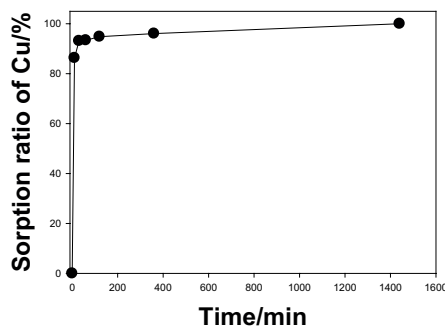


Fig. 10. Kinetics of copper ion sorption onto PEI-MNC.

isotherm in batch experiments. However, equilibrium time should be firstly measured for the adsorption isotherm study because the adsorption isotherms is the plot between the equilibrium concentration of adsorbate in the solution ( $c_e$ ) and the equilibrium amount of adsorbate adsorbed onto the sorbent ( $q_e$ ) at various initial concentration of adsorbate. Fig. 10 shows the sorption ratio of  $\text{Cu}^{2+}$  onto the PEI-MNC as a function of contact time. Initial concentration of  $\text{Cu}^{2+}$  was 10 ppm with the PEI-MNC loading of 5 mg/25 mL. The  $\text{Cu}^{2+}$  was adsorbed rapidly, and the equilibrium was established after 6 h of contact time. From the result, the subsequent adsorption

isotherm was measured at 24 h of contact time for all experiment using  $\text{Co}^{2+}$ ,  $\text{Zn}^{2+}$ , and  $\text{Cu}^{2+}$  ensuring that sorption equilibrium between sorbate and sorbent has been reached.

Fig. 11 shows a plot of the equilibrium amounts of  $\text{Cu}^{2+}$ ,  $\text{Co}^{2+}$ , or  $\text{Zn}^{2+}$  adsorbed onto the PEI-MNC prepared with different initial concentrations vs. the concentration of  $\text{Cu}^{2+}$ ,  $\text{Co}^{2+}$ , or  $\text{Zn}^{2+}$  after equilibrium, while maintaining the PEI-MNC:liquid ratio at 0.1 g/L. In general, the experimental isotherm data were usually analyzed by Langmuir isotherms. Langmuir isotherm expressions are given by the following equations:

$$1/q_e = 1/q_{\max} + 1/(q_{\max} b c_e) \quad (2)$$

where  $q_e$  and  $q_{\max}$  are the equilibrium adsorption capacity and the maximum adsorption capacity, respectively. Here,  $b$  is the Langmuir constant related to the energy of adsorption. The values of  $q_{\max}$  and  $b$  can be calculated from the intercept and slope, respectively, of the linear plot of  $1/q_e$  vs.  $1/c_e$ . It is very clear from the  $R^2$  value in Table 1 that the all adsorption process of  $\text{Cu}^{2+}$ ,  $\text{Co}^{2+}$ , and  $\text{Zn}^{2+}$  fit well to the Langmuir isotherm models. The excellent fit to the Langmuir isotherm curve suggested monolayer adsorption of heavy metals onto the PEI-MNC. From the slope and the intercept of the Langmuir plot, the values of  $q_{\max}$  for  $\text{Cu}^{2+}$ ,  $\text{Co}^{2+}$ , and  $\text{Zn}^{2+}$  were 33.11, 9.80, and 11.05 mg/g, respectively. It was found that at pH 6, the  $q_{\max}$  value for the three metal ions was  $\text{Cu}^{2+} > \text{Zn}^{2+} \approx \text{Co}^{2+}$ , implying the stronger affinity of the adsorbent for  $\text{Cu}^{2+}$  than  $\text{Zn}^{2+}$  and  $\text{Co}^{2+}$ . Contrary to other reports, the PEI-MNC has higher  $q_{\max}$  value for  $\text{Cu}^{2+}$  than those of amino-functionalized PAA-bound MNPs (12.43 mg/g) [13], chitosan-bound  $\text{Fe}_3\text{O}_4$  MNPs (21.5 mg/g) [11], and amino-functionalized magnetic nanosorbent (25.77 mg/g) [12]. This is attributed to the higher content of amine group on the PEI-MNC than those of others (amino-functionalized PAA [13], chitosan [11], and hexanediamine [12]). Although  $q_{\max}$  value for  $\text{Cu}^{2+}$  is lower than that of PEI-coated MNPs (160 mg/g) due to the lower surface area of PEI-MNC (about 200 nm in diameter) than that of single PEI-coated MNPs (50 nm in diameter) [16], the PEI-MNC covalently conjugated with PEI has better colloidal stability than PEI-coated MNPs fabricated by electrostatic conjugation between negatively charged  $\text{Fe}_3\text{O}_4$  and PEI.

The competitive adsorption among the studied metal ions was next investigated. Fig. 12 shows the adsorption results of PEI-MNC for the tri-metal solution with equal initial concentration (5 ppm) of  $\text{Cu}^{2+}$ ,  $\text{Zn}^{2+}$ , and  $\text{Co}^{2+}$ . Compared with the adsorption result for each metal ion solution (Fig. 10), the  $q_e$  value for  $\text{Co}^{2+}$  was decreased from 6.27 to 0.2 mg/g, and the  $q_e$  value for  $\text{Zn}^{2+}$  also decreased from 9.2 to 0.4 mg/g. However, the  $q_e$  value for  $\text{Cu}^{2+}$  was almost maintained even in the presence of same concentrations of  $\text{Co}^{2+}$  and  $\text{Zn}^{2+}$  (15.4 mg/g for  $\text{Cu}^{2+}$  solution and 15.0 mg/g for tri-metal solution). This result indicated that the PEI-MNC has a strong adsorption property for  $\text{Cu}^{2+}$  compared with  $\text{Zn}^{2+}$  and  $\text{Co}^{2+}$ . Although it was reported that the different adsorption behaviors between them might be relevant to the nature of metal ionic and the interaction between adsorbent and adsorbate [26], the detailed experiments need to be further investigated.

For the promising practical application, the regeneration and reusability of the PEI-MNC is very important features. According to formation of complexes ( $\text{NH}_2\text{M}^{\text{tr}}$ ) of metal ions with the free amine groups on the PEI-MNC, the protonation

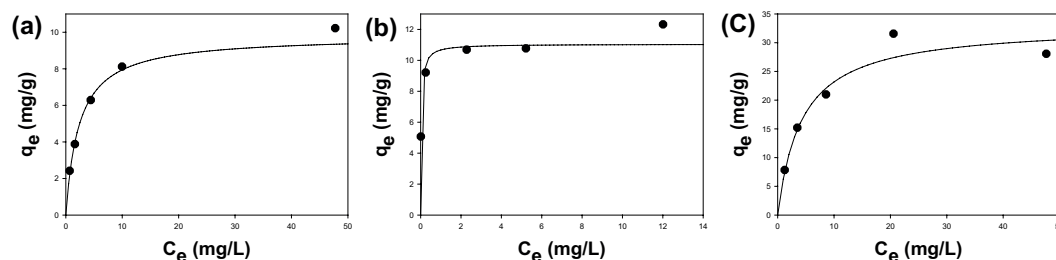


Fig. 11. The experimental isotherm data and Langmuir sorption isotherm plot for the sorption of (a) cobalt, (b) zinc, and (c) copper ions onto PEI-MNC at 293 K.

Table 1  
Parameters of the adsorption isotherms fitted by Langmuir models

	$b$	$q_{\max}$ (mg/g)	$R^2$
Co <sup>2+</sup>	0.2396	9.80	0.9949
Zn <sup>2+</sup>	0.0032	11.05	0.9848
Cu <sup>2+</sup>	0.1295	33.11	0.9940

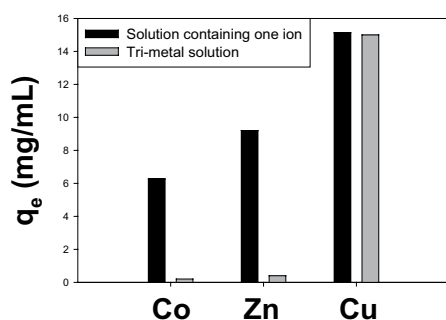


Fig. 12. Competitive adsorption of multi-metal solution.

Table 2  
Leaching of Fe and Cu ions after re-suspending the Cu<sup>2+</sup>-loaded PEI-MNC in 0.1 M HCl solution at different sonication time

Time (min)	Fe (ppm)	Cu (ppm)
2	0.51	9.01
5	0.39	10.09
10	0.43	9.52
60	0.55	10.33

of amine groups (NH<sup>3+</sup>) at lower pH can induce the desorption of Cu<sup>2+</sup> from Cu<sup>2+</sup>-loaded PEI-MNC [12,14]. Although the lower pH is better condition to protonate the amine groups, 0.1 M HCl concentration was preferred to avoid the dissolution of Fe<sub>3</sub>O<sub>4</sub> in the PEI-MNC. Table 2 and Fig. 13 show leaching amount of Fe and Cu ions, and desorption ratio of adsorbed Cu<sup>2+</sup> (after first adsorption–desorption cycle) in 0.1 M HCl solution at different sonication time intervals and indicated that Cu<sup>2+</sup> ions could be desorbed completely by only 5 min sonication in the presence of 0.1 M HCl. The concentration of free iron ions leaching from PEI-MNC in the acid solution

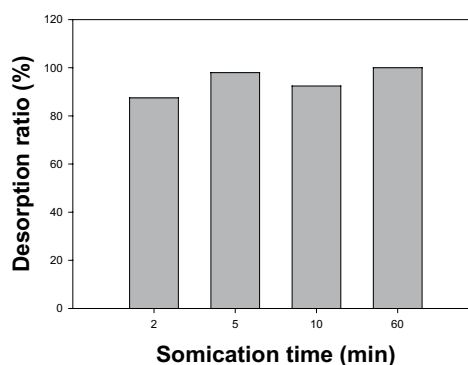


Fig. 13. Desorption ratio of adsorbed Cu<sup>2+</sup> (after first adsorption–desorption cycle) in 0.1 M HCl solution according to the sonication time.

during all desorption test is in the range of 0.39–0.55 ppm, which is almost 0.39%–0.55% of adsorbent (0.1 mg/mL). It suggests that the adsorbent is stable in the desorption process. Furthermore, the desorption and stability test of PEI-MNC in 0.1 M HCl suggest the excellent reusability of PEI-MNC. Therefore, it is believed that the PEI-MNC should be sufficiently suitable for practical applications.

#### 4. Conclusion

In this study, we fabricated a PEI-MNC through the covalent attachment of the PEI-silane on the MNC surface for the removal of heavy metal ions in water and rapid magnetic separation of the adsorbent. The PEI-MNC showed rapid magnetic separation of the adsorbent from the water. The adsorption of Cu<sup>2+</sup>, Co<sup>2+</sup>, and Zn<sup>2+</sup> was fit well to Langmuir isotherm model, and the PEI-MNC presented a preferential binding capacity of Cu<sup>2+</sup> > Zn<sup>2+</sup> ≈ Co<sup>2+</sup>. It has been also observed that PEI-MNC has strong affinity for Cu<sup>2+</sup> even in the presence of same concentrations of Co<sup>2+</sup> and Zn<sup>2+</sup>. Furthermore, the PEI-MNC displayed excellent reusability by effective desorption of Cu<sup>2+</sup> from Cu<sup>2+</sup>-loaded PEI-MNC in 0.1 M HCl solution. Therefore, it could be concluded that the PEI-MNC demonstrated good potential for the treatment of contaminated water with heavy metal ions.

#### Acknowledgments

This work was supported by the National Research Foundation of Korea (NRF) grant funded by the Korea government (MSIP) (No. 2012M2A8A5025996). We thank the staff of KBSI for their assistance with the TEM measurements.

## References

- [1] D.W. O'Connell, C. Birkinshaw, T.F. O'Dwyer, Heavy metal adsorbents prepared from the modification of cellulose: a review, *Bioresour. Technol.*, 99 (2008) 6709–6724.
- [2] Y. Chen, B. Pan, H. Li, W. Zhang, L. Lv, J. Wu, Selective removal of Cu(II) ions by using cation-exchange resin-supported polyethyleneimine (PEI) nanoclusters, *Environ. Sci. Technol.*, 44 (2010) 3508–3513.
- [3] S.E. Bailey, T.J. Olin, R.M. Brika, D.D. Adrian, A review of potentially low-cost sorbents for heavy metals, *Water Res.*, 33 (1999) 2469–2479.
- [4] R.D. Ambashta, M. Sillanpää, Water purification using magnetic assistance: a review, *J. Hazard. Mater.*, 180 (2010) 38–49.
- [5] A.-H. Lu, E.L. Salabas, F. Schüth, Magnetic nanoparticles: synthesis, protection, functionalization, and application, *Angew. Chem. Int. Ed.*, 46 (2007) 1222–1244.
- [6] H.-M. Yang, C.W. Park, P.K. Bae, T. Ahn, B.-K. Seo, B.H. Chung, J.-D. Kim, Folate-conjugated cross-linked magnetic nanoparticles as potential magnetic resonance probes for in vivo cancer imaging, *J. Mater. Chem. B*, 1 (2013) 3035–3043.
- [7] H.-M. Yang, K.-W. Lee, B.-K. Seo, J.-K. Moon, Copper ferrocyanide-functionalized magnetic nanoparticles for the selective removal of radioactive cesium, *J. Nanosci. Nanotechnol.*, 15 (2015) 1695–1699.
- [8] H.-M. Yang, S.B. Hong, Y.S. Choi, K.-W. Lee, B.-K. Seo, J.-K. Moon, Copper ferrocyanide-functionalized magnetic adsorbents using polyethyleneimine coated Fe<sub>3</sub>O<sub>4</sub> nanoparticles for the removal of radioactive cesium, *J. Nanosci. Nanotechnol.*, 16 (2016) 3067–3070.
- [9] H.-M. Yang, S.-C. Jang, S.B. Hong, K.-W. Lee, C. Roh, Y.S. Huh, B.-K. Seo, Prussian blue-functionalized magnetic nanoclusters for the removal of radioactive Cesium from water, *J. Alloy. Compd.*, 657 (2016) 387–393.
- [10] A. Bée, D. Talbot, S. Abramson, V. Dupuis, Magnetic alginate beads for Pb(II) ions removal from wastewater, *J. Colloid Interface Sci.*, 362 (2011) 486–492.
- [11] Y.C. Chang, D.H. Chen, Preparation and adsorption properties of monodisperse chitosan-bound Fe<sub>3</sub>O<sub>4</sub> magnetic nanoparticles for removal of Cu(II) ions, *J. Colloid Interface Sci.*, 283 (2005) 446–451.
- [12] Y.-M. Hao, M. Chen, Z.-B. Hu, Effective removal of Cu (II) ions from aqueous solution by amino-functionalized magnetic nanoparticles, *J. Hazard. Mater.*, 184 (2010) 392–399.
- [13] S.-H. Huang, D.-H. Chen, Rapid removal of heavy metal cations and anions from aqueous solutions by an amino-functionalized magnetic nano-adsorbent, *J. Hazard. Mater.*, 163 (2009) 174–179.
- [14] S. Singh, K.C. Barick, D. Bahadur, Surface engineered magnetic nanoparticles for removal of toxic metal ions and bacterial pathogens, *J. Hazard. Mater.*, 192 (2011) 1539–1547.
- [15] P.E. Duru, S. Bektas, Ö. Genc, S. Patir, A. Denizli, Adsorption of heavy metal ions on poly(ethylene imine)-immobilized poly(methyl methacrylate) microspheres, *J. Appl. Polym. Sci.*, 81 (2001) 197–205.
- [16] I.Y. Goon, C. Zhang, M. Lim, J.J. Gooding, R. Amal, Controlled fabrication of polyethylenimine-functionalized magnetic nanoparticles for the sequestration and quantification of free Cu<sup>2+</sup>, *Langmuir*, 26 (2010) 12247–12252.
- [17] Y. Pang, G. Zeng, L. Tang, Y. Zhang, Y. Liu, X. Lei, Z. Li, et al., Preparation and application of stability enhanced magnetic nanoparticles for rapid removal of Cr(VI), *Chem. Eng. J.*, 175 (2011) 222–227.
- [18] U. Jeong, X. Teng, Y. Wang, H. Yang, Y. Xia, Superparamagnetic colloids: controlled synthesis and niche applications, *Adv. Mater.*, 19 (2007) 33–60.
- [19] M. Ye, Q. Zhang, Y. Hu, J. Ge, Z. Lu, L. He, Z. Chen, Y. Yin, Magnetically recoverable core-shell nanocomposites with enhanced photocatalytic activity, *Chem. Eur. J.*, 16 (2010) 6243–6250.
- [20] F. Dong, W. Guo, J.-H. Bae, S.-H. Kim, C.-S. Ha, Highly porous, water-soluble, superparamagnetic, and biocompatible magnetite nanocrystal clusters for targeted drug delivery, *Chem. Eur. J.*, 17 (2011) 12802–12808.
- [21] W. Ma, S. Xu, J. Li, J. Guo, Y. Lin, C. Wang, Hydrophilic dual-responsive magnetite/PMAA core/shell microspheres with high magnetic susceptibility and pH sensitivity via distillation-precipitation polymerization, *J. Polym. Sci., Part A: Polym. Chem.*, 49 (2011) 2725–2733.
- [22] S. Nigam, K.C. Barick, D. Bahadur, Development of citrate-stabilized Fe<sub>3</sub>O<sub>4</sub> nanoparticles: conjugation and release of doxorubicin for therapeutic applications, *J. Magn. Magn. Mater.*, 323 (2005) 237–243.
- [23] R.M. Cornell, U. Schwertmann, *The iron oxide*, Wiley, Weinheim (2003).
- [24] J. Jin, F. Yang, F. Zhang, W. Hu, S.-B. Sun, J. Ma, 2,2'-(phenylazanediy) diacetic acid modified Fe<sub>3</sub>O<sub>4</sub>@PEI for selective removal of cadmium ions from blood, *Nanoscale*, 4 (2012) 733–736.
- [25] S.B. Deng, Y.P. Ting, Characterization of PEI-modified biomass and biosorption of Cu(II), Pb(II) and Ni(II), *Water Res.*, 39 (2005) 2167–2177.
- [26] Z. Reddad, C. Gerente, Y. Andres, P.L. Cloirec, Adsorption of several metal ions onto a low-cost biosorbent: kinetic and equilibrium studies, *Environ. Sci. Technol.*, 36 (2002) 2067–2073.